

Study on the Performance of $\text{AlCl}_3 / \gamma\text{-Al}_2\text{O}_3$ Catalyst with Modified $\gamma\text{-Al}_2\text{O}_3$

CAI Yan¹, ZHAN Xu-qin¹, XU Sheng¹, MI Pu-ke^{1*}, WANG Si-han², XU Xian-ming²

(1. Shanghai Key Laboratory of Advanced Polymeric Materials, Key Laboratory for Ultrafine Materials of Ministry of Education, School of Materials Science and Engineering, East China University of Science and Technology, Shanghai 200237, China;

2. Daqing Chemical Engineering Research Center, Institute of Petrochemical Engineering, PetroChina Company Limited, Daqing Heilongjiang 163714, China)

Abstract: $\gamma\text{-Al}_2\text{O}_3$ was modified with HCl and NaOH then used as supported material for preparation the catalyst $\text{AlCl}_3/\gamma\text{-Al}_2\text{O}_3$. The supported catalyst surface properties (acid center type, acid strength and acid amount) were characterized by pyridine-FTIR and pyridine-TPD. In addition, the catalytic ability of supported catalyst and its stability were evaluated by the polymerization of 1-decene. The results indicated that there were two types of acid centers on the immobilized catalyst, which were Lewis and Brønsted acid sites. Compared with $\text{AlCl}_3/\gamma\text{-Al}_2\text{O}_3$, the acid amount of NaOH modified catalyst increased 47% and the activity for 1-decene polymerization augmented 11.4%. However, as for the HCl modified catalyst, the increased value were 112% and 33.6% respectively. The acidity grew as the following order: $\text{AlCl}_3/\gamma\text{-Al}_2\text{O}_3 < \text{AlCl}_3/\gamma\text{-Al}_2\text{O}_3(\text{NaOH}) < \text{AlCl}_3/\gamma\text{-Al}_2\text{O}_3(\text{HCl})$.

Key words: modification; immobilization; γ -alumina; aluminum chloride; acid site

CLC number: O643.32

Document code: A

Environmental catalyst ($\gamma\text{-Al}_2\text{O}_3$)-O-AlCl₂ has been prepared by AlCl₃ immobilized on $\gamma\text{-Al}_2\text{O}_3$ ^[1-2], which was widely used to prepare synthetic lubricants^[3-4]. The interaction between the hydroxyl of carrier and AlCl₃ directly determined the catalyst activity, selectivity and stability. It is well known that the superficial acidic properties of catalyst are responsible for their catalytic performance, so the study of catalyst surface acidity is very important for the research of catalytic activity. It is well known the surface acidity of carrier depends on different modified methods, such as: fluorinated $\gamma\text{-Al}_2\text{O}_3$ ^[5-6], acid-modified zeolite HY^[7], chloride alumina^[8]. Liu Changkun et al^[6] found that F/ $\gamma\text{-Al}_2\text{O}_3$ had higher activity for acid catalytic reaction, both Brønsted and Lewis acid sites were found on the surface of F/ $\gamma\text{-Al}_2\text{O}_3$. The acidity of

surface hydroxyl groups (i. e., acid strength of Brønsted) increased as the amount of fluorine augmented, which attributed to the effect of high electronegativity of fluoride. The total Brønsted acidity reached a maximum when the content of fluorine with 2% ~ 3%. Wu Wei et al.^[7] found that acid strength, total acidity and the ratio of weak acid to strong acid could be modified by the chemical dealumination. David Dubé et al.^[9] reported the physical and chemical properties of immobilized AlCl₃/zeolite catalyst and characterized the acidity.

This study was about the preparation of AlCl₃/ $\gamma\text{-Al}_2\text{O}_3$ modified with HCl and NaOH. The surface acid properties (acid center type, intensity and amount) were characterized by pyridine-TPD^[10-11] and pyridine-FTIR^[12-13]. The impact of the two modified methods

Received date: 2015-03-25; **Revised date:** 2015-04-18.

Foundation: This work is supported by the National Natural Science Foundation of China (No. U1162111).

First author: Yan Cai, female, born in 1989, master, E-mail: cai1007yan@163.com.

* **Corresponding author:** Puke Mi, male, master, professor, engaged in the research of catalysts for olefin polymerization, E-mail: mpk869@163.com.

to carrier acidity and catalytic properties were also studied.

1 Experimental

1.1 Preparation of Catalyst

The γ - Al_2O_3 was impregnated with distilled water, 1.0 mol LHCl and 1.0 mol LNaOH respectively, then dried under vacuum and calcinated at $600\text{ }^\circ\text{C}$ for 6.0 h prior to use. The certain amount of supported material γ - Al_2O_3 and AlCl_3 were added to 100 mL CCl_4 under dry argon atmosphere and refluxed for 12 h, the solvent was removed by filtering and the residue was washed three times with dry CCl_4 . The grafted catalyst was obtained and stored in a Schlenk tube under dry argon atmosphere. The raw materials were supplied by Shanghai Lingfeng Chemical Reagent CO., Ltd. (China)

1.2 Catalyst Characterization

The chlorinity of the catalyst was determined by Volhard method^[14].

Adsorbed Pyridine Infrared Spectra (Pyridine-IR) was recorded on a IMPACT-420 FTIR spectrometer. The wafers were prepared in a glove box under a dry argon atmosphere. The self-supporting wafers were evacuated in situ in an IR cell at $400\text{ }^\circ\text{C}$ and 1.0×10^{-2} Pa for 3 h and 0.2 ~ 0.4 kPa pyridine was permitted to desorb at room temperature for 1 h and depressurize to 0.1 Pa at $150\text{ }^\circ\text{C}$. Then the spectra were recorded after cooling at room temperature.

The pyridine desorption experiment (pyridine-TPD) was performed on a TP-5080 adsorption instrument (Tianjin Xianquan Industry and Trade Development Co., LTD). The catalyst was prepared in a glove box under dry argon atmosphere. For pyridine-TPD, 50 mg of catalyst was treated at $25 \sim 300\text{ }^\circ\text{C}$ (ramp = $10\text{ }^\circ\text{C min}^{-1}$) and 1 h isotherm at $300\text{ }^\circ\text{C}$ under a He flow of 20 mL min^{-1} . The catalyst was cooled down to room temperature under flowing helium. The catalyst was saturated with pyridine at $120\text{ }^\circ\text{C}$ under a flow of He (15 mL min^{-1}) and pyridine (5 mL min^{-1}) for 5 min. The set up was stabilized for 3 h at $120\text{ }^\circ\text{C}$ under a flow of He (20 mL min^{-1}). The catalyst was then cooled down to room temperature. The conditions

of the desorption tests were: He (20 mL min^{-1}) temperature from $25 \sim 600\text{ }^\circ\text{C}$ (ramp = $10\text{ }^\circ\text{C min}^{-1}$). The catalyst was maintained for 5 min at $600\text{ }^\circ\text{C}$ after the end of the ramp in order to achieve desorption. A thermal conductivity detector (TCD) was used to detect.

1.3 Oligomerization of 1-decene

n-hexane (80 mL), catalyst (8g) and 1-decene (40 mL, 95%), which purchased from Tianjin Haina international trading CO., Ltd. (China), were added to three-necked flask, the mixture was increased to $80\text{ }^\circ\text{C}$ and kept for 4 h while stirring. The catalyst was filtered out and the resulting oligomer was washed sequentially with NaOH solution and distilled water. The organic phase was distilled to obtain the poly- α -olefin oil. The conversion was calculated and viscometric properties were measured using appropriate ASTM methods.

1.4 Oligomer Characterization

Gas chromatography-mass spectrometry (GC-MS) was performed on HP-6890GC-5973 MSD. A fused silica capillary column DB-5 MS ($30\text{ m} \times 0.25\text{ mm}$, $0.25\text{ }\mu\text{m}$ film thickness) was used. Helium and methane were used as the carrier and the reagent gas, respectively, for negative-ion chemical ionization. The following oven temperature program was used: 2 min at $70\text{ }^\circ\text{C}$, then an increase to $100\text{ }^\circ\text{C}$ at a rate $10\text{ }^\circ\text{C} \cdot \text{min}^{-1}$, followed by an increase to $300\text{ }^\circ\text{C}$ at a rate of $30\text{ }^\circ\text{C min}^{-1}$ for 1 h. The injection port of the GC was set at $300\text{ }^\circ\text{C}$. The maximum molecular weight that can be detected by this GC-MS instrument is approximately 500 Da.

2 Results and discussion

2.1 Pyridine-FTIR Characterization

The pyridine-FTIR of carriers and catalysts were shown in Fig. 1 with four peaks (1445 cm^{-1} , 1490 cm^{-1} , 1540 cm^{-1} , 1618 cm^{-1}). It can be seen that the shape of spectrogram is similar with different intensities. The peaks of 1445 cm^{-1} and 1540 cm^{-1} are attributed to Lewis acid sites and Brönsted acid sites respectively^[15], and the peak of 1490 cm^{-1} is attributed to both of them.

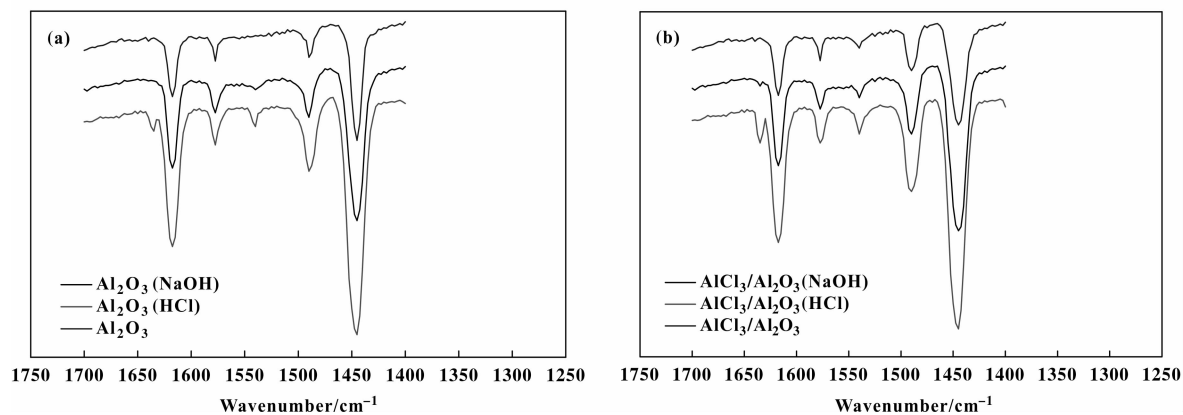


Fig. 1 Pyridine-FTIR spectra of modified carriers and catalysts:
(a) modified $\gamma\text{-Al}_2\text{O}_3$ and (b) immobilized catalyst

As shown in Fig. 1 (a), the $\gamma\text{-Al}_2\text{O}_3$ and $\gamma\text{-Al}_2\text{O}_3$ (NaOH) did not display significant pyridine FTIR signals at $1\,540\text{ cm}^{-1}$, suggesting that they have no Brönsted acid center. Moreover, among the three carries, the intensity of all pyridine-FTIR signals increased as the following order: $\gamma\text{-Al}_2\text{O}_3 < \gamma\text{-Al}_2\text{O}_3$

(NaOH) $< \gamma\text{-Al}_2\text{O}_3$ (HCl), which means that both of the strength of Lewis acid and Brönsted acid augmented with the same order. From Fig. 1 (b), the phenomenon was found for supported catalyst as well. In other words, the acidity of immobilized catalyst mainly depended on the properties of carries.

As we known, the Lambert-Beer law was employed in the form^[11,16]

$$A = \varepsilon CL \tag{1}$$

where A is the intensity of the band (integrated area, cm^{-1}), ε is the integrated extinction coefficient, C is the concentration of the vibrating species ($\text{mmol} \cdot \text{g}^{-1}$), L is the thickness of sample (mm).

The concentration of Brönsted and Lewis acid sites obtained from the bands at $1\,540\text{ cm}^{-1}$ and $1\,445\text{ cm}^{-1}$ are reported in Table 1. According to Guisnet et al.^[17], the extinction coefficients of $1\,540\text{ cm}^{-1}$ and $1\,445\text{ cm}^{-1}$ are $1.13\text{ cm } \mu\text{mol}^{-1}$ and $1.28\text{ cm } \mu\text{mol}^{-1}$ respectively.

Table 1 Acid amount of catalysts

Item	Composition/w%		Acid amount/($\text{mmol} \cdot \text{g}^{-1}$)		
	Cl	OH	L	B	L+B
$\text{AlCl}_3/\gamma\text{-Al}_2\text{O}_3$	0	0	1.055	0.055	1.110
$\text{AlCl}_3/\gamma\text{-Al}_2\text{O}_3(\text{NaOH})^{\text{a}}$	0	1.4	1.569	0.062	1.631
$\text{AlCl}_3/\gamma\text{-Al}_2\text{O}_3(\text{HCl})^{\text{a}}$	2.8	0	2.204	0.149	2.353

a. The mass fraction of NaOH and HCl were about 3%.

As show in Table 1, the acid amount of Lewis acid center is much greater than that of Brönsted acid. The value of L+B implied that the total acid amount of NaOH modified catalyst increased 47% and that of $\text{AlCl}_3/\gamma\text{-Al}_2\text{O}_3(\text{HCl})$ increased 112% compared with $\text{AlCl}_3/\gamma\text{-Al}_2\text{O}_3$. It means the catalyst acid intensity (Lewis and Brönsted acids) enhanced significantly after $\gamma\text{-Al}_2\text{O}_3$ modified with HCl, which indicated that

the HCl improved the surface acidity of catalyst dramatically, we call it HCl effect. We consider that the HCl effect comes from the high electronegativity of chlorine. Some hydroxyl on the carrier surface was replaced by chlorine^[6] and the strong inductive effect of Al-Cl bond weakened even broken the Al-OH bond and strong Lewis acid sites Al^{\oplus} was formed. Moreover, the strong inductive effect of Al-Cl bond also lead to strong

deprotonation of molecules of coordinatively bonded water, i. e., which caused an increase in the Brönsted acidity^[8]. However, when the $\gamma\text{-Al}_2\text{O}_3$ modified by NaOH, the surface hydroxyl concentration increased and Lewis Al^\oplus sites formed by surface dehydration at

higher temperature calcination^[8], the Lewis acid sites are more than that of $\gamma\text{-Al}_2\text{O}_3$ but lower than that of $\gamma\text{-Al}_2\text{O}_3(\text{HCl})$. Therefore, the presumed modified carrier structure was shown in Fig. 2.

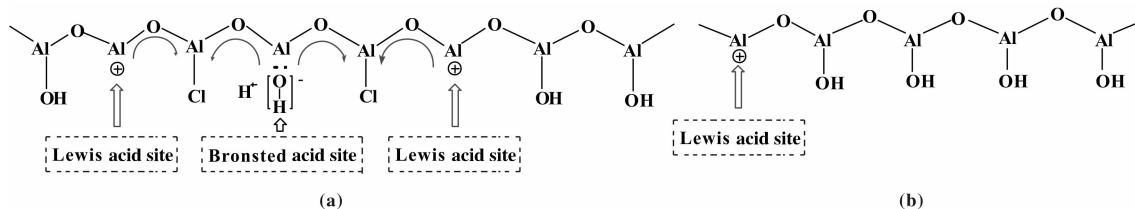


Fig. 2 Surface structure of modified $\gamma\text{-Al}_2\text{O}_3$: (a) $\gamma\text{-Al}_2\text{O}_3(\text{HCl})$ and (b) $\gamma\text{-Al}_2\text{O}_3(\text{NaOH})$

During the immobilization process, the active species $-\text{AlCl}_2$ and $-\text{AlCl}$ were produced when AlCl_3 reacted with surface hydroxyl, and the $-\text{AlCl}_2$ is primary species^[1]. The Lewis acid sites Al^\oplus reacted with the

Cl of AlCl_3 and then the Al coordinated to oxygen atoms of adjacent hydroxyl, at last Brönsted acid sites was formed^[9]. Thus, the proper immobilized catalyst surface structure was shown in Fig. 3.

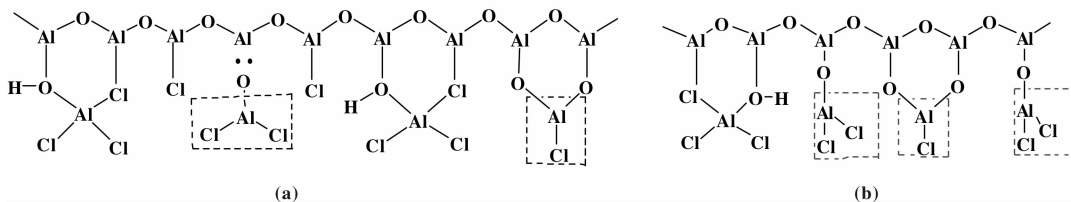


Fig. 3 Surface structure of immobilized catalyst: (a) $\text{AlCl}_3/\gamma\text{-Al}_2\text{O}_3(\text{HCl})$ and (b) $\text{AlCl}_3/\gamma\text{-Al}_2\text{O}_3(\text{NaOH})$

2.2 Pyridine-TPD Characterization

The density of acid sites was determined by pyridine-TPD and the result was shown in Fig. 4. The incorporation of AlCl_3 by a grafting reaction on modified Al_2O_3 created two types of acid sites. According to literature, the peak at 200°C and $360 \sim 400^\circ\text{C}$ were attributed to Lewis acid sites^[18] and Brönsted acid sites respectively^[9,19].

The combination energy of pyridine to acid center was determined by the acidity strength, and could be characterized by desorption temperature^[20]. That is to say, the stronger the acidity, the greater the binding energy, and the desired desorption temperature is higher^[21]. Fig. 4 showed the desorption temperature increased in according with the $\text{AlCl}_3/\gamma\text{-Al}_2\text{O}_3$, $\text{AlCl}_3/\gamma\text{-Al}_2\text{O}_3(\text{NaOH})$, $\text{AlCl}_3/\gamma\text{-Al}_2\text{O}_3(\text{HCl})$ order, which confirmed our assumption about the surface structure of immobilized catalyst and that the acidity of HCl modified catalyst is the most among three immobilized catalysts.

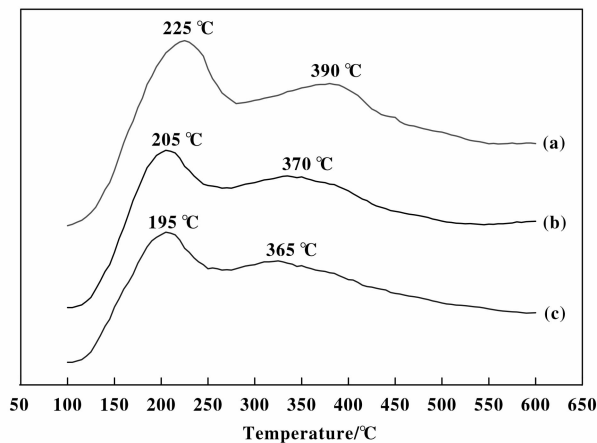


Fig. 4 Pyridine-TPD of immobilized catalyst: (a) $\text{AlCl}_3/\gamma\text{-Al}_2\text{O}_3(\text{HCl})$, (b) $\text{AlCl}_3/\gamma\text{-Al}_2\text{O}_3(\text{NaOH})$ and (c) $\text{AlCl}_3/\gamma\text{-Al}_2\text{O}_3$

2.3 Oligomerization behaviors

The properties and composition distribution of oligomers are shown in Table 2.

Table 2 Effect of supported catalysts on 1-decene oligomerization reaction

Catalyst	$K_v/(\text{mm}^2 \cdot \text{s}^{-1})^b$			Product composition/% ^c			
	Conv. /% ^a	40 °C	100 °C	Di-	Tri-	Tetra-	Penta-
$\text{AlCl}_3/\gamma\text{-Al}_2\text{O}_3$	56.8	28.5	5.6	27.9	30.6	25.4	16.1
$\text{AlCl}_3/\gamma\text{-Al}_2\text{O}_3(\text{NaOH})$	63.2	33.8	6.6	18.2	29.6	32.7	19.5
$\text{AlCl}_3/\gamma\text{-Al}_2\text{O}_3(\text{HCl})$	75.8	21.4	4.7	40.7	29.2	19.2	11.0

a. Conversion of 1-decene; b. Kinetic viscosity of oligomer; c. Determined by GC-Mass.

Table 2 showed the conversion of 1-decene increases as the following order: $\text{AlCl}_3/\gamma\text{-Al}_2\text{O}_3 < \text{AlCl}_3/\gamma\text{-Al}_2\text{O}_3(\text{NaOH}) < \text{AlCl}_3/\gamma\text{-Al}_2\text{O}_3(\text{HCl})$, and the corresponding conversion augmented from 56.8% to 63.2% and 75.8%, this order was just like to that of acidity. The catalytic activity increased with the

increasing of acidity. However, the viscosity of oligomer by $\text{AlCl}_3/\gamma\text{-Al}_2\text{O}_3(\text{HCl})$ was the lowest and the component of that was primarily dimers and trimers, where as oligomer by $\text{AlCl}_3/\gamma\text{-Al}_2\text{O}_3(\text{NaOH})$ was mainly made up of trimers and tetramers (Fig. 5).

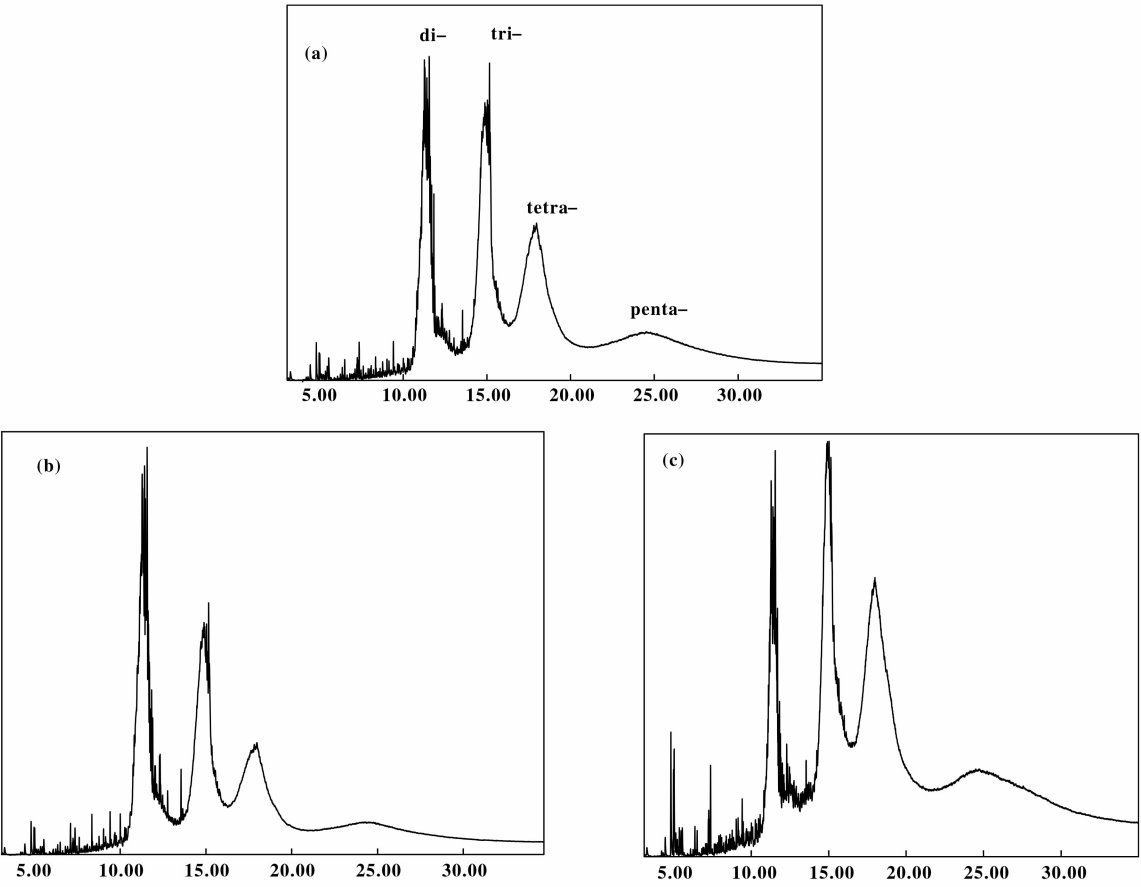


Fig. 5 GC-MS spectra of oligomers: (a) $\text{AlCl}_3/\gamma\text{-Al}_2\text{O}_3$, (b) $\text{AlCl}_3/\gamma\text{-Al}_2\text{O}_3(\text{HCl})$ and (c) $\text{AlCl}_3/\gamma\text{-Al}_2\text{O}_3(\text{NaOH})$

From the polymerization results, it was found that the catalytic activity was mainly controlled by acidity, when $\text{AlCl}_3/\gamma\text{-Al}_2\text{O}_3(\text{HCl})$ was used, the reaction speed and conversion varied directly with acidity and inversely with the viscosity of oligomer. As for

$\text{AlCl}_3/\gamma\text{-Al}_2\text{O}_3(\text{NaOH})$, the surface hydroxyl concentration of carrier improved, which means there are more AlCl_3 loading to carrier by the reaction of AlCl_3 to hydroxyl, and the value of activated center augmented, thus the catalytic activity increased accordingly. The

acid amount and acid strength of $\text{AlCl}_3/\gamma\text{-Al}_2\text{O}_3$ (NaOH) was lower than $\text{AlCl}_3/\gamma\text{-Al}_2\text{O}_3$ (HCl), hence the conversion decreased and oligomer viscosity increased.

The stability of the immobilized catalysts were measured in a batch reactor. The results shown in Fig. 6.

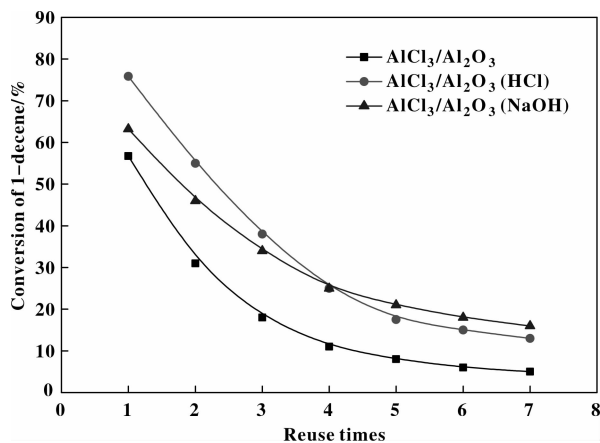


Fig. 6 The stability of immobilized aluminium chloride catalyst

Figure 6 reveals that the conversion of 1-decene markedly decreases during the first four reuse times. After that, the conversion of 1-decene decreases slightly. Two reasons account for this phenomenon. One is the pore-clogging effect, the other is the destruction of active centers with H_2O or alcohols^[22].

The decreasing rate of 1-decene conversion with three catalysts is $\text{AlCl}_3/\gamma\text{-Al}_2\text{O}_3 < \text{AlCl}_3/\gamma\text{-Al}_2\text{O}_3$ (HCl) $< \text{AlCl}_3/\gamma\text{-Al}_2\text{O}_3$ (NaOH). It means that the catalysts stability is $\text{AlCl}_3/\gamma\text{-Al}_2\text{O}_3 < \text{AlCl}_3/\gamma\text{-Al}_2\text{O}_3$ (HCl) $< \text{AlCl}_3/\gamma\text{-Al}_2\text{O}_3$ (NaOH). Han^[23] have found that the stability of catalysts depends on the surface area and pore volume rather than acidity. Acidity does not benefit the lifetime of the catalyst. So with the modification of NaOH and HCl, the pore volume and surface area increase, thus the stability of catalysts increases.

3 Conclusions

The modification of support affect its surface acid properties (acid center type, acid strength and acid amount), there by altering the surface acidity of catalyst and the catalytic activity. Ultimately influence the oli-

gomer composition and viscosity.

The strength of carrier acidity can be changed by the way to modification, so as to regulate the catalyst acid intensity. Finally it achieves the purpose of adjusting catalytic activity and kinematic viscosity of the product.

The stability of the catalysts used for the oligomerization of 1-decene is not depend on the acidity.

References:

- [1] Lu P F, Jiang L, Mi P K, *et al.* Structure of immobilized AlCl_3 catalyst with Al_2O_3 as support[J]. *Petrochem Technol*, 2010, **39**(6): 616-619.
- [2] Wang N N, Jiang S, Ji M, He M, *et al.* Preparation of immobilized AlCl_3 catalyst for 1-Decene polymerization [J]. *Petrochem Technol*, 2006, **35**(5): 479-482.
- [3] a. Cai TX, He M. New approaches to immobilization of aluminum chloride on γ -alumina and its regeneration after deactivation[J]. *Catal Lett*, 2003, **86**(1/3): 17-23.
b. Ge Y Y, Jia Z Q, Zhao L L, *et al.* Evolution of acidity properties and catalytic performance for tetrahydrofuran polymerization of $\text{SiO}_2\text{-Al}_2\text{O}_3$ during heat treatment process[J]. *J Mol Catal (China)* (分子催化), 2013, **27**(2): 166-172.
c. Wang H N, Guo Z W, Yang S H, *et al.* Dehydrogenation of cyclohexane with alkaline-earth metal modified V/K- $\gamma\text{-Al}_2\text{O}_3$ catalyst[J]. *J Mol Catal (China)* (分子催化), 2013, **27**(3): 256-265.
- [4] a. Cai TX, He M, Shi X Z. New approaches to immobilization of aluminium chloride on $\gamma\text{-Al}_2\text{O}_3$ [J]. *Chem J Chin Univer*, 2001, **22**(8): 1385-1387.
b. Kang L N, Guo J Y, Zhang H X, *et al.* Activity and stability of Ni/ $\text{SiO}_2\text{-Al}_2\text{O}_3$ catalyst in the aqueous phase hydrogenation system[J]. *J Mol Catal (China)* (分子催化), 2014, **28**(2): 119-125.
c. Ma X Y, Chen X H, Chen Q F. Study on catalytic performances of $\text{La}_2\text{O}_3/\gamma\text{-Al}_2\text{O}_3$ in reaction of citral and acetone[J]. *J Mol Catal (China)* (分子催化), 2014, **28**(3): 251-258.
- [5] Bautista F M, Campelo J M, Garcia A, *et al.* Fluoride and sulfate treatment of $\text{AlPO}_4\text{-Al}_2\text{O}_3$ Catalysts. I. Structure, Texture, surface acidity and catalytic performance in cyclohexene conversion and cumene cracking [J]. *J Catal*, 1994, **145**(1): 107-125.
- [6] Liu C K, Yie Z H. NMR and FTIR Characterization of surface Acidity of Fluorinated $\gamma\text{-Al}_2\text{O}_3$ [J]. *Chem J Chin*

- Univer*, 2002, **23**(10): 1952–1955.
- [7] Wu G, Zhou D P, Han X, *et al.* Study on surface acidity of modified HY zeolite by NH_3 -TPD method[J]. *Chem Adhe*, 2006, **28**(1): 17–19.
- [8] Sharanda L F, Shimansky A P, Kulik T V, Chuiko A A. Study of acid-base surface properties of γ -alumina oxide [J]. *Coll Sur A: Physicochem Engin Asp*, 1995, **105**(2/3): 167–172.
- [9] Dubé David, Royer Sébastien, On Do Trong, *et al.* Aluminum chloride grafted mesoporous molecular sieves as alkylation catalysts[J]. *Micro Mes Mater*, 2005, **79**(1/3): 137–144.
- [10] Neumann G T, Hicks J C. Dual roles of steam in the dry gel synthesis of mesoporous ZSM-5[J]. *Cry Grow & Des*, 2013, **13**(4): 1535–1542.
- [11] Wu L P, Li X J, Yuan Z H, Chen Y. The fabrication of TiO_2 -supported zeolite with core/shell heterostructure for ethanol dehydration to ethylene [J]. *Catal Commun*, 2009, **11**(1): 67–70.
- [12] Benaliouche F, Boucheffa Y, Ayrault P, *et al.* NH_3 -TPD and FTIR spectroscopy of pyridine adsorption studies for characterization of Ag- and Cu-exchanged X zeolites[J]. *Micro Mes Mater*, 2008, **111**(1/3): 80–88.
- [13] Montanari T, Finocchio E, Busca G. Infrared spectroscopy of heterogeneous catalysts: acidity and accessibility of acid sites of faujasite-type solid acids [J]. *J Chem Phys*, 2011, **115**(4): 937–943.
- [14] Potgieter S S, Potgieter J H, Panicheva S. Investigation into methods of chloride analysis of South African cement and cement-related materials with low chloride concentration[J]. *Mater Stru*, 2004, **37**(3): 155–160.
- [15] Sage V, Clark J H, Macquarrie D J. Cationic polymerization of styrene using mesoporous silica supported aluminum chloride[J]. *J Mol Catal A: Chem*, 2003, **198**(1/2): 349–358.
- [16] Martins G V A, Berlier G, Bisio C, *et al.* Quantification of brønsted acid sites in microporous catalysts by a combined FTIR and NH_3 -TPD study [J]. *J Phys Chem C*, 2008, **112**(18): 7193–7200.
- [17] Guisnet M, Ayrault P, Coutanceau C, *et al.* Acid properties of dealuminated beta zeolites studied by IR spectroscopy[J]. *J. Chem Soc Faraday Trans*, 1997, **93**(8): 1661–1665.
- [18] Zhai S R, Wei W, Wu D, Sun Y H. Synthesis, characterization and catalytic activities of mesoporous AlMSU-X with wormhole-like framework structure [J]. *Catal Lett*, 2003, **89**(3/4): 261–267.
- [19] Dapurkar S E, Selvam P. Mesoporous H-AlMCM-48: highly efficient solid acid catalyst [J]. *Appl Catal A: Gen*, 2003, **254**(2): 239–249.
- [20] Resini C, Montanari T, Nappi L, *et al.* Selective catalytic reduction of NO_x by methane over Co-H-MFI and Co-H-FER zeolite catalysts: characterisation and catalytic activity[J]. *J Catal*, 2003, **214**(2): 179–190.
- [21] Xu Y M, Shen BX, He J H, Luo X H. Study of surface acidity of $\gamma\text{-Al}_2\text{O}_3$ support by PASCA and NH_3 -TPD[J]. *J Instru Anal*, 2006, **25**(1): 41–44.
- [22] Cai TX, He M, Shi X Z, Wang X P. Influence of geometric structure of immobilized aluminum chloride catalyst on catalytic property in isobutene polymerization[J]. *Chin Chem Lett*, 2001, **12**(7): 647–650.
- [23] Han M H, Xu C, Lin J, *et al.* Alkylation of benzene with long-chain olefins catalyzed by fluorinated β zeolite [J]. *Catal Lett*, 2003, **86**(1/3): 81–86.

$\gamma\text{-Al}_2\text{O}_3$ 改性对 $\text{AlCl}_3/\gamma\text{-Al}_2\text{O}_3$ 催化剂性能的影响

蔡 艳¹, 詹续芹¹, 许 胜¹, 米普科^{1*}, 王斯晗², 徐显明²

(1. 华东理工大学 材料科学与工程学院, 上海市先进聚合物材料重点实验室, 超细材料制备与应用教育部重点实验室, 上海 200237;

2. 中国石油天然气股份有限公司 石油化工研究院 大庆化工研究中心, 黑龙江 大庆 163714)

摘要: 采用 HCl 和 NaOH 改性 $\gamma\text{-Al}_2\text{O}_3$ 载体制备 $\text{AlCl}_3/\gamma\text{-Al}_2\text{O}_3$ 固载催化剂, 用吡啶-FTIR 和吡啶-TPD 技术分析了催化剂的表面酸性(酸中心类型、酸强度和酸量), 并以 1-癸烯齐聚作为探针反应, 研究了催化剂的稳定性以及催化剂对聚合反应的影响。结果表明, 催化剂含有两种酸类型, 即 Lewis 酸和 Brønsted 酸, 与未改性的催化剂相比, 氢氧化钠改性载体制备的催化剂, 酸量增大了 47%, 催化剂催化 1-癸烯的齐聚反应活性增加了 11.4%; 而经盐酸改性制备的催化剂酸量增大 112%, 催化剂的活性增加了 33.6%。酸强度依 $\text{AlCl}_3/\gamma\text{-Al}_2\text{O}_3$, $\text{AlCl}_3/\gamma\text{-Al}_2\text{O}_3$ (NaOH), $\text{AlCl}_3/\gamma\text{-Al}_2\text{O}_3$ (HCl) 的顺序增强。

关键词: 改性; 固载; γ -氧化铝; 三氯化铝; 酸性位